Comprehensive Nonlinearity Simulation of Different Types and Modes of HEMTs with Respect to Biasing Conditions

M. M. Karkhanehchi, A. Ammani

Abstract—A simple analytical model has been developed to optimize biasing conditions for obtaining maximum linearity among lattice-matched, pseudomorphic and metamorphic HEMT types as well as enhancement and depletion HEMT modes. A nonlinear current-voltage model has been simulated based on extracted data to study and select the most appropriate type and mode of HEMT in terms of a given gate-source biasing voltage within the device so as to employ the circuit for the highest possible output current or voltage linear swing. Simulation results can be used as a basis for the selection of optimum gate-source biasing voltage for a given type and mode of HEMT with regard to a circuit design. The consequences can also be a criterion for choosing the optimum type or mode of HEMT for a predetermined biasing condition.

Keywords—Biasing, characteristic, linearity, simulation.

I. INTRODUCTION

WIDE band-gap HEMTs are emerging as excellent candidates for radio frequency power amplifiers (PAs) because of their high power handling capabilities [1]-[3]. Their demonstrated low-noise and high breakdown characteristics show their potential for protection-circuit-free low-noise amplifiers (LNAs) [4], [5]. HEMTs operate in two biasing modes [6], [7]. The development of monolithically integrated enhancement and depletion-mode high electron mobility transistors (E/D-HEMTs) is of considerable interest for high-speed, low-power communication systems [8].

Also according to lattice constant utilized in the layers of a HEMT, three types are distinguishable known as lattice-matched HEMT (LHEMT), pseudomorphic HEMT (PHEMT) and metamorphic HEMT (MHEMT).

In LHEMT lattice constants of the two materials employed in both sides of the hetero structure are the same [9] while in PHEMT the lattice constants are slightly different [10]-[12] and in MHEMT the two lattice constants are significantly different. Hence in this type of HEMT, it is routine to grow a buffer layer between the two materials for compensating and moderating the rather large difference [13]-[15].

M. M. Karkhanehchi is Corresponding Author and with the Electrical Engineering Department, Faculty of Engineering, Razi University, Tagh-E-Bostan, Kermanshah, 67149, Iran.(phone: +98 9123783947; fax: +98 8314283261; e-mail: :mkarkhanehchi@razi.ac.ir).

A. Ammani is with the Electrical Engineering Department, Razi University, Tagh-E-Bostan, Kermanshah, 67149, Iran. (e-mail: amir.ammani@yahoo.com).

Most of electronic circuits operate in environments being exposed to temperature variations and so temperature fluctuations affects biased voltage causing the displacement of operating point. On the other side, one of the important parameters within designation of electronic circuits is reaching the maximum output current and voltage swing. Therefore utilizing one circuit optimally and economically upon taking maximum symmetric output swing requires to be biased in which maximum linear symmetric range is gained. This factor depicts its vitality within the construction of integrated circuits in architecture level and higher because nonlinearities superposition affects output swing dramatically through various transistors of an IC [16].

Here through extracting current and voltage data, graphs of different types of high electron mobility transistors have been analyzed with regard to distinguish nonlinear behavior of their characteristics [17], [18]. Then voltage-current pinch-off point has been probed as one of the most important nonlinear design characteristic and the best type among LHEMT , PHEMT and MHEMT as well as the optimum biasing have been represented successively. Eventually in order to achieve optimum biasing, nonlinear behavior has been investigated within temperature fluctuation considerations and with the aim of maximum symmetric swing.

II. THEORETICAL ANALYSIS

Many RF circuits are approximated by linear and consequently small signal models, but nonlinear features of the semiconductor devices affect the proposed small signal model. On the other hand while the amplitude of the input signal increases, the gain of the device or circuit starts to vary nonlinearly. Indeed this nonlinearity can be ascribed to change in small signal gain via input signal level and this obviously denotes that for very large input amplitudes, the circuit or device gain tends to zero. This means that gain is inversely varied with respect to input amplitudes. In RF and digital circuits this effect is defined as the input amplitude in which small signal gain experiences one decibel reduction and the voltage is named as one-decibel pinch-off point or voltage. This point is known to be a standard or yardstick to compare the degree of linearity of a RF or digital circuit or device. To compute one decibel pinch-off voltage of different types of HEMTs, first suppose that the current versus voltage considering the most applicable signal nonlinearity is given by:

$$i_{ds} = \alpha_1 v_{ds} + \alpha_2 v_{ds}^2 + \alpha_3 v_{ds}^3 + \alpha_4 v_{ds}^4$$
$$+ \alpha_5 v_{ds}^5 + \alpha_6 v_{ds}^6 + \alpha_7 v_{ds}^7 \tag{1}$$

For sinusoidal state, substitute $v_{ds} = A\cos\omega t$ where A is output voltage signal amplitude. So Eq. (1) is rearranged to:

$$i_{ds} = \alpha_1 A\cos\omega t + \alpha_2 A^2 \cos^2\omega t + \alpha_3 A^3 \cos^3\omega t$$
$$+ \alpha_4 A^4 \cos^4\omega t + \alpha_5 A^5 \cos^5\omega t + \alpha_6 A^6 \cos^6\omega t \tag{2}$$
$$+ \alpha_7 A^7 \cos^7\omega t$$

Now using half angle mathematical relations gives:

$$i_{ds} = \alpha_1 A\cos\omega t$$
$$+ \alpha_2 \frac{A^2}{2}(1 + \cos 2\omega t)$$
$$+ \alpha_3 \frac{A^3}{4}(3\cos\omega t + \cos 3\omega t)$$
$$+ \alpha_4 \frac{A^4}{8}(3 + 4\cos 2\omega t + \cos 4\omega t)$$
$$+ \alpha_5 \frac{A^5}{16}(10\cos\omega t + 5\cos 3\omega t + \cos 5\omega t)$$
$$+ \alpha_6 \frac{A^6}{32}(10 + 15\cos 2\omega t + 6\cos 4\omega t + \cos 6\omega t)$$
$$+ \alpha_7 \frac{A^7}{64}(35\cos\omega t + 21\cos 3\omega t + 7\cos 5\omega t$$
$$+ \cos 7\omega t) \tag{3}$$

Rearranging the similar expressions gives:

$$i_{ds} =$$
$$[\alpha_1 + \frac{3}{4}\alpha_3 A^2 + \frac{5}{8}\alpha_5 A^4 + \frac{35}{64}\alpha_7 A^6]A\cos\omega t$$
$$+ [\frac{1}{2}\alpha_2 A^2 + \frac{1}{2}\alpha_4 A^4 + \frac{15}{32}\alpha_6 A^6]\cos 2\omega t$$
$$+ [\frac{1}{4}\alpha_3 A^3 + \frac{5}{16}\alpha_5 A^5 + \frac{21}{64}\alpha_7 A^7]\cos 3\omega t$$
$$+ [\frac{3}{8}\alpha_4 A^4 + \frac{3}{16}\alpha_6 A^6]\cos 4\omega t$$
$$+ [\frac{1}{16}\alpha_5 A^5 + \frac{7}{64}\alpha_7 A^7]\cos 5\omega t$$
$$+ [\frac{1}{32}\alpha_6 A^6]\cos 6\omega t + [\frac{1}{64}\alpha_7 A^7]\cos 7\omega t$$
$$+ [\frac{1}{2}\alpha_2 A^2 + \frac{3}{8}\alpha_4 A^4 + \frac{5}{16}\alpha_6 A^6] \tag{4}$$

Substituting $v_{ds} = A\cos\omega t$ back and due to the importance of only the first coefficient in our computations gives:

$$i_{ds} = [\alpha_1 + \frac{3}{4}\alpha_3 A^2 + \frac{5}{8}\alpha_5 A^4 + \frac{35}{64}\alpha_7 A^6]v_{ds} + \ldots \tag{5}$$

In linear state in which current-voltage relationship is $i_{ds} = \alpha_1 v_{ds}$ in which α_1 is indeed small signal gain. So linear small signal gain is given by

$$G_L = \alpha_1 \tag{6}$$

Comparing the above equation with linear state denotes the small signal gain to be:

$$G_{NL} = \alpha_1 + \frac{3}{4}\alpha_3 A^2 + \frac{5}{8}\alpha_5 A^4 + \frac{35}{64}\alpha_7 A^6 \tag{7}$$

According to the definition of one-decibel pinch-off point, it is mathematically formulated as the point in which:

$$|G_{NL}|_{dB} = |G_L|_{dB} - 1dB \tag{8}$$

This can be changed to logarithm form as:

$$20\log|G_{NL}| = 20\log|G_L| - 1 \tag{9}$$

As we defined previously, A is output voltage signal amplitude and the amplitude which satisfies Eq. (9) is in fact one-decibel pinch-off voltage and from now on is depicted by A_{1-dB} for simplicity. Substituting Eq. (6), Eq. (7) to Eq. (9) gives:

$$20\log\left|\alpha_1 + \frac{3}{4}\alpha_3 A_{1-dB}^2 + \frac{5}{8}\alpha_5 A_{1-dB}^4 + \frac{35}{64}\alpha_7 A_{1-dB}^6\right|$$
$$= 20\log|\alpha_1| - 1 \tag{10}$$

To simplify Eq. (10) let:

$$1db = 20\log 10^{\frac{1}{20}} = 20\log 10^{0.05} \tag{11}$$

It gives:

$$20\log\left|\alpha_1 + \frac{3}{4}\alpha_3 A_{1-dB}^2 + \frac{5}{8}\alpha_5 A_{1-dB}^4 + \frac{35}{64}\alpha_7 A_{1-dB}^6\right|$$
$$= 20\log|\alpha_1| - 20\log 10^{0.05} = 20\log\frac{|\alpha_1|}{10^{0.05}} \tag{12}$$

Finally, omitting 20log from both sides of Eq. (12) gives:

$$\left|\alpha_1 + \frac{3}{4}\alpha_3 A_{1-dB}^2 + \frac{5}{8}\alpha_5 A_{1-dB}^4 + \frac{35}{64}\alpha_7 A_{1-dB}^6\right|$$
$$= \frac{|\alpha_1|}{10^{0.05}} \tag{13}$$

Solving this nonlinear equation while we have coefficient α_j gives the one-decibel pinch-off voltage. In this paper Eq. (13) has been solved for all types of HEMT.

III. DATA ANALYSIS

In order to simulate one-decibel pinch-off voltage of different types of HEMTs, we need to initially simulate their related output current-voltage graphs. These graphs have been simulated according to experimental data [7], [19] and [20] and are presented subsequently for miscellaneous sorts of HEMTs. In Figs .1and .2, a HEMT has been biased at two different range of gate bias and indeed two modes emerge. In

Figs .3, .4 and .5, there different heterostructures in which a high-electron mobility transistor is constructed have been under test to achieve its I-V characteristic.
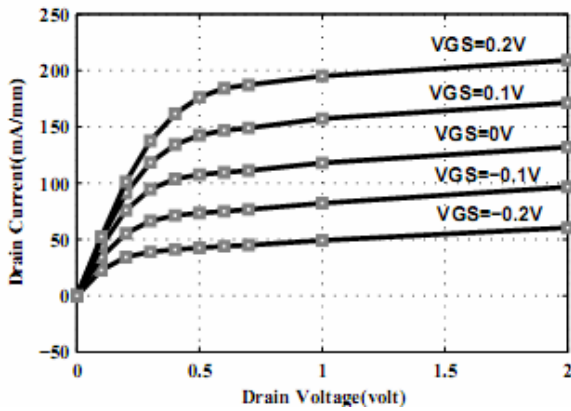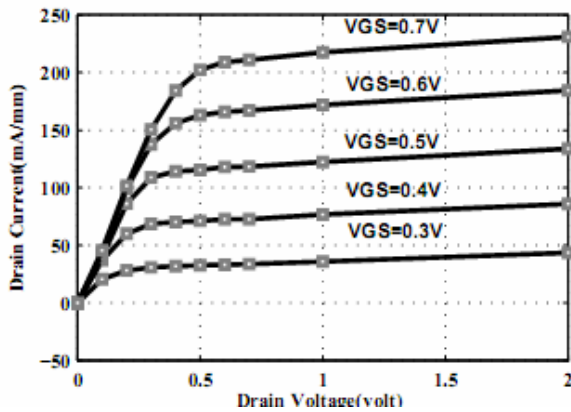

Fig. 1 I-V characteristic of DHEMT
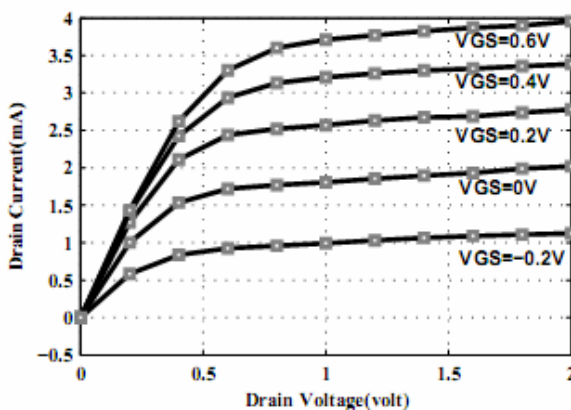

Fig. 2 I-V characteristic of EHEMT

Fig. 3 I-V characteristic of LHEMT

In Fig. 1, knee region starts nearly more than VDS=0.5v while in Fig. 2, knee happens at a drain-source biasing voltage less than 0.5 volt. Hence depletion-mode shows a wider small-voltage linear region enabling the device swing at bigger

small signal amplitudes and being more reliable with respect to drain-source bias deviations.

In Fig. 3, knee area is between VDS=0.5v, VDS=1v and for drain voltages more than 1 volt, the characteristic looks like a line with good approximation.
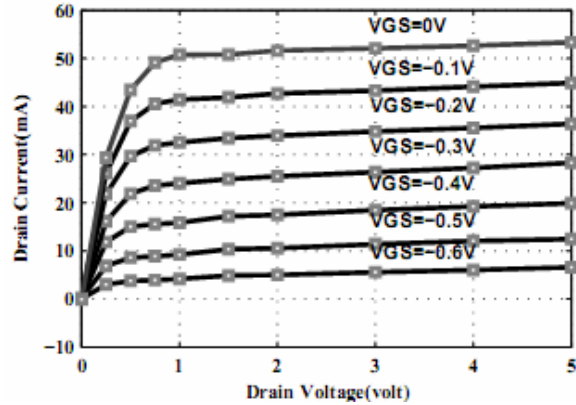

Fig. 4 I-V characteristic of PHEMT

In Fig .4, knee area is located at drain voltages less than 1 volt while in Fig. 5, seems to be near one or more. This demonstrates that MHEMT has better low-bias reliability with respect to drain voltage deviations than PHEMT.
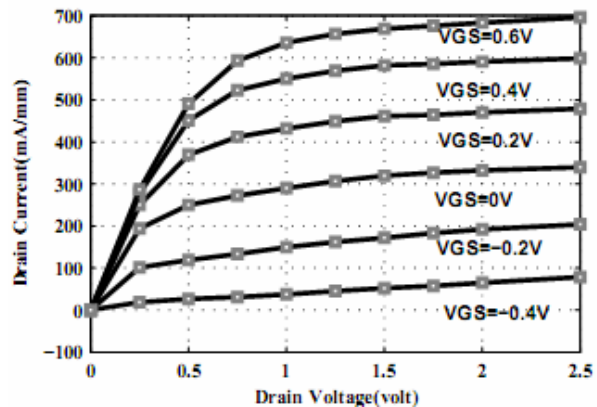

Fig. 5 I-V characteristic of MHEMT

Extracting related polynomial for each I-V characteristic, gives the coefficients of the nonlinear equation. These coefficients are presented for one sample gate-source voltage per graph and are summarized in two following tables. First table is related to Depletion-mode HEMT(D-HEMT) and Enhancement-mode HEMT(E-HEMT) while the second is related to Lattice-matched-type HEMT(L-HEMT), Pseudomorphic-type HEMT(P-HEMT), Metamorphic-type HEMT(M-HEMT).

In Table I, sign of coefficients are the same for both modes from α_1 to α_4 while from α_5 to α_7, the signs are opposite for two different modes. It indicates that for coefficients more than α_4, characteristic behavior of modes are inverse with respect to each other, meaning that if current is increasing in

terms of a given range of voltage for depletion mode, it is decreasing for enhancement mode and vice-versa.

TABLE I
COEFFICIENTS RELATED TO HEMT MODES

α	D-HEMT at V_{GS}=0.2volt	E-HEMT at V_{GS}=0.7volt
α_1	0.0462	0.3194
α_2	0.1283	1.8780
α_3	-0.7602	-5.5260
α_4	1.5788	4.1487
α_5	-1.6858	1.2879
α_6	0.8991	-2.6665
α_7	-0.1824	0.7762

TABLE II
COEFFICIENTS RELATED TO HEMT TYPES

α	L-HEMT at V_{GS}=0.6volt	P-HEMT at V_{GS}=0volt	M-HEMT at V_{GS}=0.6volt
α_1	6.4277	160.2668	1.1247
α_2	9.4791	-198.8929	0.8160
α_3	-36.1485	124.1993	-3.8826
α_4	41.3965	-41.3838	4.4068
α_5	-23.2079	7.1856	-2.4179
α_6	6.4877	-0.5662	0.6614
α_7	-0.7229	0.0122	-0.0722

In Table II, the sign of all coefficients in second column are opposite to the signs corresponding to the coefficients in first or third column and therefore PHEMT have a perfectly distinctive behavior in comparison with LHEMT and MHEMT.

IV. RESULTS AND DISCUSSION

According to the current-voltage characteristic of depletion mode HEMT, It is clear that maximum channel current takes place near zero gate-source biases. As the gate voltage decreases from zero, current follows alike till reaching threshold current which indeed is the minimum current flown in the channel, pointing to normally-closed behavior of DHEMT as a key while EHEMT behaves vice-versa. For slightly positive bias voltages in D-mode current flows through channel as well. On the other hand, the important feature of D-mode is its capability to be utilized as E-mode too, which introduces DHEMT as an applicable device in RF invertors and complimentary HEMT logical and digital architectures but an EHEMT can not be biased in D-mode.
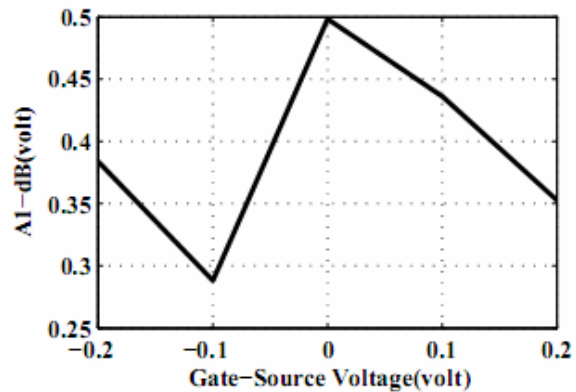

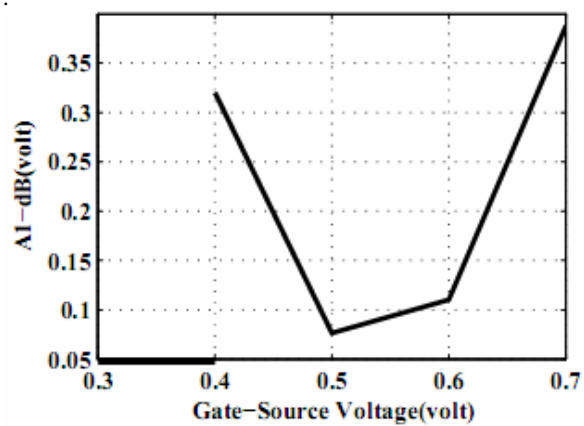Fig. 6 One-decibel pinch-off voltage versus gate-source bias voltage in DHEMT

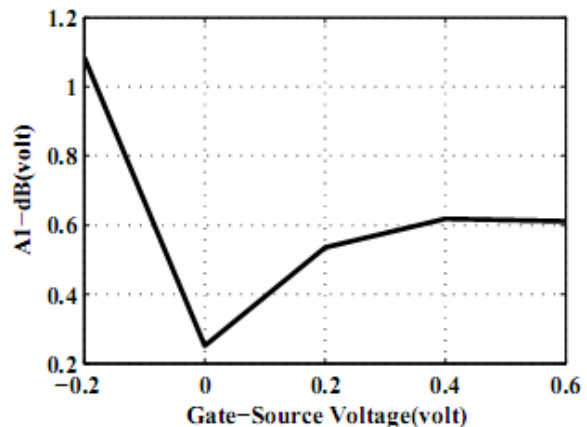Fig. 7 One-decibel pinch-off voltage versus gate-source bias voltage in EHEMT

Fig. 8 One-decibel pinch-off voltage versus gate-source bias voltage in LHEMT

In Fig. 6, with increasing bias voltage more than V_{GS}=0, one decibel pinch-off voltage decreases which this inverse dependence shows that for V_{GS}>0, the more the electronic circuit bias the more linear range of DHEMT characteristic

and hence less harmonic components emerge in output terminals besides the higher efficiency is conducted.

In Fig.7, for $V_{GS}<0.4$volt, gain or voltage reduction is less than one decibel so at this range of EHEMT current-voltage characteristic, larges reachable circuit linearity is achieved.

For $0.5>V_{GS}>0.4$, A_{1-dB} is inversely related to V_{GS} and as voltage increases at this range one decibel reduction occurs at smaller voltage such that the linear area of the characteristic will diminish and therefore this range is not appropriate for biasing . For $V_{GS}>0.5$volt, the larger gate bias voltage the larger one-decibel pinch-off point(A_{1-dB}). On the other hand through increasing gate bias voltage, one decibel attenuation occurs at higher gains or input voltages at $V_{GS}>0.5$volt and therefore the circuit linearity and maximum symmetric output current and voltage are augmented.

In Fig.8, A_{1-dB} is inversely depending on V_{GS} for negative gate-source voltages. As bias gets more negative, one decibel attenuation takes place at higher V_{DS} and therefore linear range of LHEMT I-V characteristic raises and on the other hand more negative biasing brings about larger maximum output swing. For $V_{GS}>0$volt first as bias increases A_{1-dB} increases too denoting better linearity but as approaching $V_{GS}=0.4$volt, A_{1-dB} starts to change negligibly meaning that for $V_{GS}>0.4$volt, one decibel attenuation is approximately constant and hence $V_{GS}>0.4$volt is the best range for biasing LHEMT.
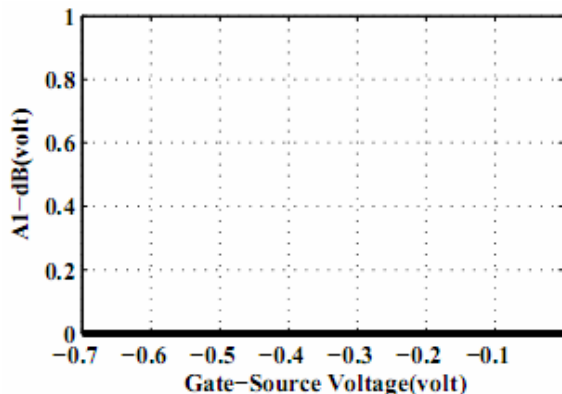
Fig. 9 One-decibel pinch-off voltage versus gate-source bias voltage in PHEMT

In Fig.9 gain and voltage reduction are less than 1-db for all biasing conditions showing that PHEMT among types of transistors has the highest linear range and widest symmetric output swing and due to this reason PHEMT seems to be one of the best candidate for integrated circuits and architectures.

In Fig.10 for $V_{GS}<0.2$volt, one decibel attenuation is less than one decibel and so the best biasing range to achieve highest possible output swing. For $0.4>V_{GS}>0.2$, A_{1-dB} is inversely depending on V_{GS} and so as bias increases A_{1-dB} happens at higher V_{GS} causing higher linearity and swing and therefore MHEMT has the highest efficiency and suitability for IC technology at this range of biasing . For $V_{GS}>0.4$volt,

one decibel attenuation is inversely related to gate voltage meaning the more the gate voltage the less linearity and swing and it is because A_{1-dB} occurs at smaller V_{GS}. Therefore $V_{GS}>0.4$volt is not offered for circuit biasing.

The overall results are summarized in following tables where we can get the tips for optimum biasing and device type or mode.
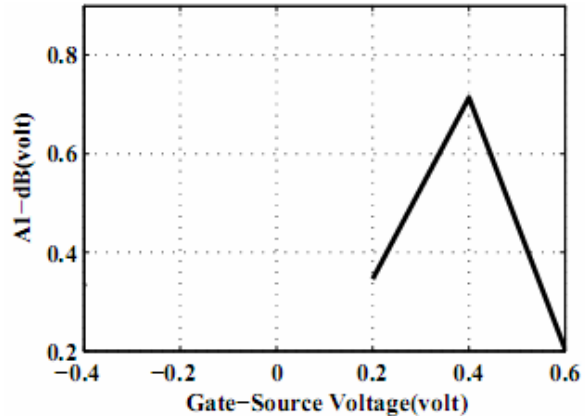
Fig. 10 One-decibel pinch-off voltage versus gate-source bias voltage in MHEMT

TABLE III
OPTIMUM BIAS RANGE VERSUS TRANSISTOR TYPE

Type of HEMT	L-HEMT	P-HEMT	M-HEMT
optimum bias range(volt)	$V_{GS}>0$	$V_{GS}<0$	$0<V_{GS}<0.2$

TABLE IV
OPTIMUM TRANSISTOR TYPE VERSUS BIAS RANGE

Bias range(volt)	$V_{GS}<0$	$0<V_{GS}<0.2$	$V_{GS}>0$
Optimum type of HEMT	P-HEMT	M-HEMT	L-HEMT

TABLE V
OPTIMUM BIAS RANGE VERSUS TRANSISTOR MODE

Mode of HEMT	D-HEMT	E-HEMT
Optimum bias range(volt)	Bias-insensitive	$0<V_{GS}<0.4$

In Table III, we have supposed that the type of HEMT technology has been chosen according to other applications and factors previously and we are looking for the best biasing condition.

In Table IV, we have supposed that the biasing range has been chosen according to other applications and factors previously and we are looking for the best type of HEMT technology.

In Table V, we have supposed that the mode of HEMT technology has been chosen according to other applications and factors previously and we are looking for the best biasing range in which highest linearity and swing is achieved as mentioned formerly.

These tables can be interpreted for application of HEMTs besides other applications of it [21]-[23].

V. CONCLUSION

Through this paper a good comparison was carried out for the simulated one-decibel pinch-off voltage point versus biasing conditions. The technique evaluates the degree of linearity in RF circuits and digital architecture design more accurately. The maximum symmetric output current and voltage swing was studied by this method where RF output linear swing range was obtained at three various and empirical types of HEMTs and conventional HEMT modes as well. It was shown that DHEMT is not sensitive to gate-source bias and PHEMT is suitable for negative biasing while LHEMT, MHEMT and EHEMT are good candidates for positive bias ranges as demonstrated.

REFERENCES

[1] S. T. Sheppard, K. Doverpike, W. L. Pribble, S. T. Allen, and J. W. Palmour, "High power microwave GaN/AlGaN HEMTs on silicon carbide," IEEE Electron Device Lett., Vol. 20, no. 4, pp. 161-163, Apr. 1999.

[2] V. Tilak, B. Green, V. Kaper, H. Kim, T. Prunty, J. Smart, J. Shealy, and L. Eastman, "Influence of barrier thickness on the high-power performance of AlGaN/GaN HEMTs, " IEEE Electron Device Lett., Vol. 22, no. 11, pp. 504-506, Nov. 2001.

[3] K. H. G. Duh, P. C. Chao, S. M. J. Liu, P. Ho, M. Y. Kao, and J. M. Ballingall, "A supper low-noise $0.1 \mu m$ T-gate InAlAs/InGaAs/InP HEMT," IEEE Microwave Guided Wave Lett., Vol. 1, pp. 114-116, May 1991.

[4] P. M. Smith, S. J. Liu, M. Y. Kao, P.Ho, S. C. Wang, K. H. G. Duh, S. T. Fu, and P. C. Chao, "Wide-band high-efficiency InP-based power HEMT with 600 GHz f_{max}," IEEE Microwave Guided Wave Lett., Vol. 5, pp. 230-232, July 1995.

[5] W. Saito, Y. Takada, M. Kuraguchi, K. Tsuda, I. Omura, T.Ogura, and H. Ohashi, "High breakdown voltage AlGaN-GaN power-HEMT design and high current density switching behavior,"IEEE Trans. Electron Devices, Vol. 50, no. 12, pp. 2528-2531, Dec. 2003.

[6] M. A. Khan, Q. Chen, C. J. Sun, J. W. Yang, M. Blasingame, M. S. Shur, and H. Park, "Enhancement and depletion mode GaN/AlGaN heterostructure field effect transistors ," Appl. Phys. Lett., Vol. 68, no. 4, pp. 514-516, Jan. 1996.

[7] A. Mahajan, P. Fay, M. Arafa, and I. Adesia, "Integration of InAlAs/InGaAs/InP enhancement-and depletion-mode high electron mobility transistors for high-speed circuit applications," IEEE Trans. Electron. Devices, Vol. 45, no. 1, pp. 0018-9383, Jan. 1998.

[8] J. S. Moon et al., "Submicron enhancement-mode AlGaN/GaN HEMTs" in proc. 60th Device Research Conf., Santa Barba, CA, 2002, pp. 23-25.

[9] Y. Yamashita, A. Endoh, K. Shinohara, M. Higashiwaki, K. Hikosaka, T. Mimura, S. Hiyamizu and T. Matsui, "Ultra-short 25-nm-gate lattice-matched InAlAs/InGaAs HEMTs within the range of 400GHz cut-off frequency," IEEE Electron. Dev. Lett., Vol. 22, pp. 367-369, Aug. 2001.

[10] L. D. Nguyen, A. S. Brown, M. A. Thompson, and L. M. Jelloian, "50-nm self-aligne-gate pseudomorphic AlInAs/GaInAs high-electron mobility transistors" IEEE Trans. Electron Device, Vol. 39, pp. 2007-2014, Sept. 1992.

[11] Y. C. Lin, E. Y. Chang, G. J. Chen, H. M. Lee, G. W. Huang, D. Biswas, and C. Y. Chang, "InGaP/InGaAs PHEMT with high IP3 for low noise applications," Electron. Lett., Vol. 40, no. 12, pp. 777-778, Jun. 2004.

[12] K. H. Yu, H. M. Chuang, K. W. Lin, S. Y. Cheng, C. C. Cheng, J. Y. Chen, and W. C. Liu, "Improved tempreture-dependent performances of a novel InGaP-InGaAs-GaAs double channel pseudomorphic high electron mobility transistor (DC-PHEMT)," IEEE Trans. Electron. Devices, Vol. 49, no. 10, pp. 1687-1693, Oct. 2002.

[13] C. S. Whelan, P. F. Marsh, W. E. Hoke, and T. E. Kazior, "GaAs metamorphic HEMT : the ideal candidate for high performance, millimeter wave low noise and power applications," GaAs Manufacturing Technology Conference, Washington, USA, pp. 237-240, May 1-4. 2000.

[14] P. C. Chao, K. C. Hwang, D. W. Tu, J. S. M. Liu, O. Tang, and K. Nichols, "Very high efficiency and low cost power metamorphic HEMT MMIC technology," GaAs Manufacturing Technology Conference, Washington, USA, pp. 57-60, May 1-4. 2000.

[15] M. Chertouk, F. Benkhelifa, M. Damman, M. Walther, K. Kohler, and G. Weimann, "Metamorphic InAlAs/InGaAs MMIC technology on GaAs substrate from promise to reality," GaAs Manufacturing Technology Conference, Washington, USA, pp. 233-236, May 1-4. 2000.

[16] M. Miller ,M.Golio, B. Bechwith, E. Arnold, D. Halchin, S. Ageno, S. Dorn, " Choosing an optimum large signal model for GaAs MESFETs AND HEMTs " ,IEEE MTT-S 1990 .

[17] I. Angelov, H. Zirath, and N. Rorsman, "A New Empirical Non-linear Model for HEMT and MESFET Devices,"IEEE Trans. on MTT, Vol. 40, 1992.

[18] Takashi Aigo, Mitsuhiko Goto, Yasumitsu Ohta, Aiji Jono, Akiyoshi Tachikawa, and Akihiro Moritani, "Threshold voltage uniform and characterization of microwave perfonance for GaAs/AlGaAs high electron mobility trasistors grown on Si substrate ",IEEE Trans. Electron. Devices. Vol. 43, no. 4, April. 1996.

[19] T. Aigo, M. Goto, Y. Ohta, A. Jono, A. Tachikawa, and A. Moritani, "Threshold voltage uniformity and characterization of microwave performance for GaAs/AlGaAs high electron-mobility transistors grown on Si substrates," IEEE Trans. Electron Device, Vol. 43, no. 4, Apr. 1996.

[20] F. Benkhelifa, M. Chertouk, M. Dammann, H. Massler, M. Walther, G. Weinmann, "High performance metamorphic HEMT with 0.25 μm refractory metal gate on 4 GaAs substrate," GaAs Manufacturing Technology Conference, Washington, USA, 2001.

[21] R. Khanna, L. Stafford, L. F. Voss, S. J. Pearton, H. T. Wang, T. Anderson, S-C. Hung, and F. Ren, "Aging and stability of GaN high electron mobility transistors and light-emitting diodes with TiB_2- and Ir-based contacts," IEEE Trans. Device and Materials Reliability, Vol. 8, no. 2, Jun. 2008.

[22] V. Kumar, D. H. Kim, A. Basu, and I. Adesia, "0.25 μm self-aligned AlGaN/GaN high electron mobility transistors" IEEE Electron Device Lett., Vol. 29, no. 1, Jan. 2008.

[23] M. Damman et al , "Reliability and degradation mechanism of AlGaN/GaN HEMTs for next generation mobile communication systems" Microelectronics Reliability, Vol. 49, pp. 474-477, 2009.